Optical Diffusion of Focused Beam Wave Pulses in Discrete Random Media

Arnold D. Kim[a] and Akira Ishimaru[b]

[a]Department of Applied Mathematics, University of Washington, Seattle, WA 98195, USA

[b]Department of Electrical Engineering, University of Washington, Seattle, WA 98195, USA

ABSTRACT

In this paper we present a theoretical study of focused beam wave pulse propagation and diffusion in highly scattering discrete random media. By using Wigner distributions, we calculate an explicit closed-form expression for the reduced intensity of focused beam waves. From this analysis, we find that the extent to which the reduced intensity focuses depends upon the attenuation it experiences from scattering and absorption. We then solve the diffusion equation for continuous wave sources and delta function input pulses to examine the spatial and temporal spreading of beam wave pulses. Through numerical approximations to the obtained solutions, we find that focusing effects of the diffuse intensity are negligible. Finally, we compare these results to those of collimated beam waves and pulsed plane waves. Through these comparisons, we determine that the spatial spreading of focused beams is similar to that of collimated beams, and the temporal spreading of the focused beam wave pulse is similar to that of plane wave pulses.

Keywords: Optical diffusion, radiative transport, focused beams, Wigner distributions.

1. INTRODUCTION

Optical beam wave propagation in discrete random media has attracted considerable amounts of interest among those working in optical imaging of biological media, and optical communication and remote sensing through fog and rain. For these applications, a thorough knowledge of the spatio-temporal spreading of the beam wave pulse is necessary. There has been much theoretical work done on these problems using the parabolic equation technique[1,2] where the scattering is mainly confined to the forward direction. However, for discrete random media where particle sizes vary on the order of a wavelength or smaller, scattering occurs over large angles and the parabolic approximation is not valid. Therefore, one must use the theory of radiative transport to investigate these problems.

The theory of radiative transport models classical wave propagation in discrete random media.[1] This theory describes the transport of energy that is emitted, scattered and absorbed in a medium containing a random distribution of scattering particles.[3] In the limit when a significant amount of multiple scattering takes place with little absorption, the diffuse component of the specific intensity develops a nearly isotropic angular distribution and the corresponding radiative transport equation reduces to a simpler diffusion equation for the angularly averaged diffuse intensity.[4–7] This approach to studying highly scattering random media has lead to a number of fundamental results that have been successfully applied to biomedical optics,[8] for example.

The Wigner distribution was originally constructed to examine quantum mechanical systems in phase space.[9] It is also a useful tool for studying classical wave propagation since its properties are very similar to those of the specific intensity of transport theory. Because the Wigner distribution is constructed from the fundamental wave field, it provides one with a mathematical tool to bridge fundamental wave fields to the specific intensity of the phenomenological theory of radiative transport. This relationship of the Wigner distribution to transport theory is well known and has been studied by a number of authors.[10–12]

After giving a brief overview of optical diffusion in random media, we examine focused beam waves and their corresponding Wigner distributions in order to determine the correct form for the reduced intensity. Then we calculate the solution to the diffusion equation for continuous wave sources and delta function input pulses. From these investigations, we examine the temporal and spatial spreading of the pulse.

Further author information: (Send correspondence to Arnold D. Kim)
Department of Applied Mathematics; Box 352420; University of Washington; Seattle, WA 98195-2420; Phone: (206) 221-5167, Fax: (206) 685-1440, E-mail: adkim@amath.washington.edu

2. THE THEORY OF RADIATIVE TRANSPORT

Radiative transport theory models classical wave propagation in a scattering and absorbing medium.[3] The fundamental quantity of transport theory is the specific intensity, $I(\bar{\mathbf{x}}, \hat{\mathbf{s}}, t)$, which depends on a position vector, $\bar{\mathbf{x}} = (x_1, x_2, x_3)$, time, t, and a unit directional vector, $\hat{\mathbf{s}}$. It is a non-negative and real-valued function for all space and directions. The specific intensity in the narrow-band limit is governed by the space-time radiative transfer equation,

$$\frac{1}{c}\frac{\partial}{\partial t} I(\bar{\mathbf{x}}, \hat{\mathbf{s}}, t) + \hat{\mathbf{s}} \cdot \nabla I(\bar{\mathbf{x}}, \hat{\mathbf{s}}, t) + \gamma_t I(\bar{\mathbf{x}}, \hat{\mathbf{s}}, t) = \frac{\gamma_s}{4\pi} \int_{4\pi} p(\hat{\mathbf{s}}, \hat{\mathbf{s}}') I(\bar{\mathbf{x}}, \hat{\mathbf{s}}', t) d\Omega(\hat{\mathbf{s}}'), \tag{1}$$

where c is the constant wave speed, γ_t is the extinction coefficient, γ_s is the scattering coefficient, $p(\hat{\mathbf{s}}, \hat{\mathbf{s}}')$ is the phase function and $d\Omega(\hat{\mathbf{s}}')$ is the differential element on the unit sphere in direction $\hat{\mathbf{s}}'$. Upon obtaining a solution to the radiative transport equation, we can calculate the average intensity by integrating the specific intensity over all directions,

$$\frac{1}{4\pi} \int_{4\pi} I(\bar{\mathbf{x}}, \hat{\mathbf{s}}, t) d\Omega(\hat{\mathbf{s}}) = U(\bar{\mathbf{x}}, t). \tag{2}$$

This average intensity is proportional to the energy density. A quantity that is often used in biomedical optics applications is the radiant energy fluence rate defined as

$$\Psi(\bar{\mathbf{x}}, t) = 4\pi U(\bar{\mathbf{x}}, t) = \int_{4\pi} I(\bar{\mathbf{x}}, \hat{\mathbf{s}}) d\Omega(\hat{\mathbf{s}}). \tag{3}$$

In addition, we can calculate the flux vector by integrating the product of the specific intensity and the direction vector over all directions,

$$\int_{4\pi} I(\bar{\mathbf{x}}, \hat{\mathbf{s}}, t)\, \hat{\mathbf{s}}\, d\Omega(\hat{\mathbf{s}}) = \mathbf{F}(\bar{\mathbf{x}}, t). \tag{4}$$

2.1. The Diffusion Approximation

The specific intensity is normally expressed as the sum of the reduced intensity, I_{ri}, and the diffuse intensity, I_d. When the specific intensity undergoes a significantly large amount of scattering, its reduced intensity exponentially decays according to the extinction theorem and its diffuse component's angular distribution becomes nearly isotropic or nearly independent of $\hat{\mathbf{s}}$. This limiting process towards an isotropic specific intensity is the main assumption of the diffusion approximation.[1,4–7] From this assumption, we can expand the diffuse intensity into an asymptotic series of Legendre functions,

$$I_d(\bar{\mathbf{x}}, \hat{\mathbf{s}}, t) \sim U(\bar{\mathbf{x}}, t) + \frac{3}{4\pi} \mathbf{F}(\bar{\mathbf{x}}, t) \cdot \hat{\mathbf{s}} + \cdots \tag{5}$$

leading to a diffusion equation for the average intensity of the form,[7]

$$\frac{1}{c}\frac{\partial}{\partial t} U(\bar{\mathbf{x}}, t) - D\nabla^2 U(\bar{\mathbf{x}}, t) + \gamma_a U(\bar{\mathbf{x}}, t) = \gamma_s U_{ri}(\bar{\mathbf{x}}, t). \tag{6}$$

The diffusion coefficient, $D = \ell_{tr}/3$, is defined in terms of the transport mean free path, ℓ_{tr}. The scattering coefficient is denoted by γ_s and the absorption coefficient, γ_a, is related to the total and scattering coefficients by $\gamma_a = \gamma_t - \gamma_s$. The right hand side is proportional to the average reduced intensity denoted by $U_{ri}(\bar{\mathbf{x}}, t)$. From the solution of the diffusion equation, we can compute the diffuse flux vector by the approximate equality[7]

$$\mathbf{F}(\bar{\mathbf{x}}, t) \cong -cD\nabla U(\bar{\mathbf{x}}, t). \tag{7}$$

For a continuous wave source, the corresponding diffusion equation is

$$-D\nabla^2 U(\bar{\mathbf{x}}) + \gamma_a U(\bar{\mathbf{x}}) = \gamma_s U_{ri}(\bar{\mathbf{x}}). \tag{8}$$

Although there exist many discrepancies among various researchers regarding the "proper" form of the diffusion equation, its boundary conditions and its coefficients,[13–16] we have chosen to adhere to the commonly used diffusion theory presented in a recent review by van Rossum and Nieuwenhuizen.[7] In this proceeding, we intend to keep the analysis and results as general as possible so that they can be easily adapted to other diffusion theories. Discrepancies between the variety of different diffusion theories most often occur at early times proximal to sources where the diffusion approximation is not valid.[16] Therefore, we shall restrict our attention to long times and large distances away from the source where all diffusion theories seem to agree with reasonably well with each other.[16]

3. THE REDUCED INTENSITY FOR FOCUSED BEAM WAVES

A scalar, time-harmonic wave field of a high-frequency Gaussian beam wave with a quadratic phase front propagating in the $\hat{z}$ direction takes the form[17]

$$\phi(\bar{\mathbf{x}}_T, x_3) = \frac{A_o}{\alpha\beta(x_3)} \exp\left[-\frac{x_T^2}{\beta(x_3)} + ik_o n x_3\right]. \tag{9}$$

The beam wave parameters are defined as

$$\alpha = 1/W_o^2 + ik_o/2R_o, \quad \text{and} \quad \beta(x_3) = 1/\alpha + i2x_3/k_o n,$$

where W_o is the beam waist, k_o is the free space propagation constant, and R_o is the phase front's radius of curvature.

To consider these focused beam waves in the theory of radiative transport and thus, the diffusion approximation, we must understand the behavior of the reduced intensity of these beam waves. In anticipation of using the Wigner distribution of this wave field to derive the reduced intensity, we consider propagation in a lossy medium with a complex refractive index, $n = n' + in''$. For the reduced intensity, the attenuation of the wave field is due to extinction and the expression, $\gamma_t = 2k_o n''$, relates the imaginary part of the refractive index used above to the extinction coefficient.[4]

3.1. The Wigner Distribution

The Wigner distribution was originally constructed as an auxiliary phase-space distribution function for quantum mechanical systems.[9] However, it is also useful as a tool for studying classical wave propagation, and there exists a relationship between the Wigner distribution and the specific intensity that is well established.[10–12] Let us summarize some of these important relationships.

The Wigner distribution of a time-harmonic wave field, $\phi(\bar{\mathbf{x}})$, is defined as

$$\mathcal{W}(\bar{\mathbf{x}}, \bar{\mathbf{k}}) = (2\pi)^{-3} \int_{\mathbb{R}^3} d^3\bar{\mathbf{y}} \exp[i\bar{\mathbf{k}} \cdot \bar{\mathbf{y}}]\, \phi^*(\bar{\mathbf{x}} + \bar{\mathbf{y}}/2)\phi(\bar{\mathbf{x}} - \bar{\mathbf{y}}/2). \tag{10}$$

Integrating the Wigner distribution with respect to the wave vector, $\bar{\mathbf{k}} = (k_1, k_2, k_3)$, yields the energy density of the wave,

$$\int_{\mathbb{R}^3} \mathcal{W}(\bar{\mathbf{x}}, \bar{\mathbf{k}})\, d^3\bar{\mathbf{k}} = |\phi(\bar{\mathbf{x}})|^2. \tag{11}$$

Calculating the first moment of the Wigner distribution with respect to the wave vector yields the Poynting vector,

$$\int_{\mathbb{R}^3} \mathcal{W}(\bar{\mathbf{x}}, \bar{\mathbf{k}})\, \bar{\mathbf{k}}\, d^3\bar{\mathbf{k}} = \frac{1}{2i} \left[\phi^*(\bar{\mathbf{x}})\nabla\phi(\bar{\mathbf{x}}) - \phi(\bar{\mathbf{x}})\nabla\phi^*(\bar{\mathbf{x}})\right]. \tag{12}$$

Furthermore, the Wigner distribution is a real-valued function for all $\bar{\mathbf{x}}$ and $\bar{\mathbf{k}}$.

With these properties, one may be inclined to interpret the Wigner distribution as a wave-vector dependent energy density that is equivalent to the specific intensity, but the Wigner distribution is not a non-negative function, in general. Therefore, the Wigner distribution cannot be entirely interpreted as this wave-vector dependent energy density. However, the Wigner distribution becomes a non-negative function in the high-frequency asymptotic limit.[12] For example, consider a plane wave with constant amplitude, A_o, propagating in free space in the $\hat{\mathbf{s}}$ direction,

$$\phi(\bar{\mathbf{x}}) = A_o \exp[ik_o \hat{\mathbf{s}} \cdot \bar{\mathbf{x}}]. \tag{13}$$

Upon substituting this plane wave expression into the definition of the Wigner distribution, we obtain

$$\mathcal{W}(\bar{\mathbf{x}}, \bar{\mathbf{k}}) = |A_o|^2 \delta(\bar{\mathbf{k}} - k_o\hat{\mathbf{s}}). \tag{14}$$

Similarly, a high-frequency wave with a slowly varying complex amplitude, $A(\bar{\mathbf{x}})$, and phase, $S(\bar{\mathbf{x}})$, is

$$\phi^{(\epsilon)} \sim A(\bar{\mathbf{x}}) \exp[iS(\bar{\mathbf{x}})/\epsilon] \quad \text{as } \epsilon \to 0^+, \tag{15}$$

where ϵ is a small, positive parameter used to evaluate the high-frequency limit. The high-frequency asymptotic Wigner distribution[12] takes the form

$$\mathcal{W}(\bar{\mathbf{x}}, \bar{\mathbf{k}}) \sim |A(\bar{\mathbf{x}})|^2\, \delta(\bar{\mathbf{k}} - \nabla S(\bar{\mathbf{x}})). \tag{16}$$

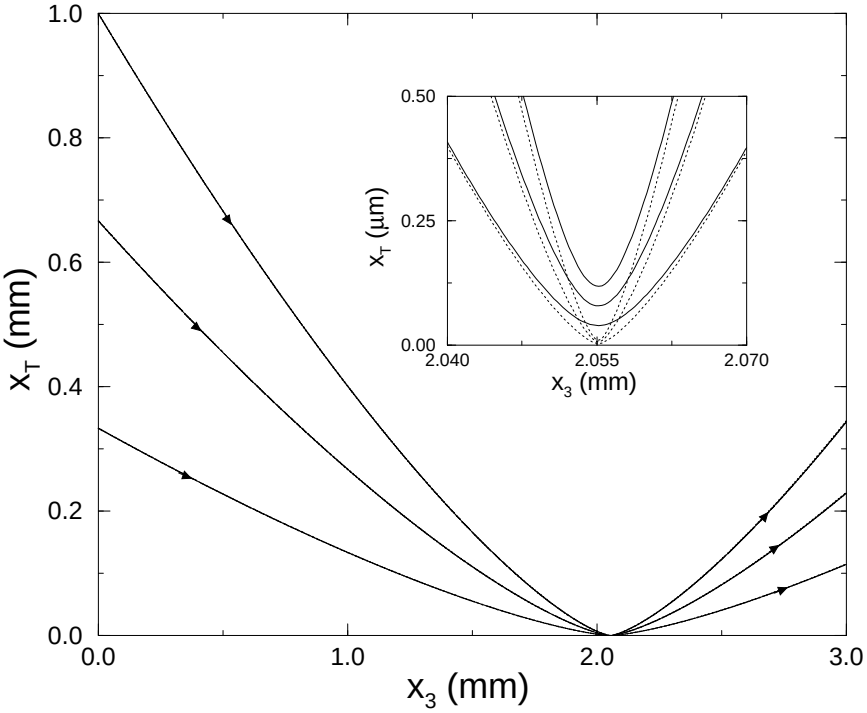

Figure 1. Ray paths of the Wigner distribution starting from $x_T = W_o/3,\, 2W_o/3$ and W_o. Here $W_o = 1\,mm$, $R_o = 1.5\,mm$, $n' = 1.37$ and $\lambda = 467\,nm$. Dotted lines correspond to propagation in free space and solid lines correspond to propagation with $\gamma_t = 42\,mm^{-1}$. The inset plot is a close-up showing the defocusing due to extinction.

3.2. Wigner Distribution of Focused Beam Waves

By rearranging terms in the beam wave defined in (9), we find that the amplitude is

$$A(\bar{\mathbf{x}}) = \frac{A_o}{\alpha\beta(x_3)} \exp\left[-f_r(x_3)\frac{x_T^2}{W_o^2} - k_o n'' x_3\right]. \tag{17}$$

In addition, we find the phase is

$$S(\bar{\mathbf{x}}) = k_o n' x_3 - f_i(x_3)\frac{x_T^2}{W_o^2}. \tag{18}$$

Here, we define

$$f_r(x_3) = \mathsf{Re}\left[\frac{Wo^2}{\beta(x_3)}\right] = d^{-1}(x_3)\left(1 + \frac{x_3}{n' z_o}\frac{n''}{n'}\frac{1 + z_o^2/R_o^2}{1 + n''^2/n'^2}\right), \tag{19}$$

$$f_i(x_3) = \mathsf{Im}\left[\frac{Wo^2}{\beta(x_3)}\right] = d^{-1}(x_3)\left(\frac{z_o}{R_o} - \frac{x_3}{n' z_o}\frac{1 + z_o^2/R_o^2}{1 + n''^2/n'^2}\right), \tag{20}$$

$$z_o = k_o W_o^2/2, \tag{21}$$

and

$$d(x_3) = 1 + \frac{x_3^2}{n'^2 z_o^2}\frac{1 + z_o^2/R_o^2}{1 + n''^2/n'^2} + 2\frac{x_3}{n' z_o}\frac{1}{1 + n''^2/n'^2}\left(\frac{n''}{n'} - \frac{z_o}{R_o}\right). \tag{22}$$

Upon substituting these expressions above as well as $n'' = \gamma_t/2k_o$ into the high-frequency asymptotic form of the Wigner distribution, we obtain

$$\mathcal{W}(\bar{\mathbf{x}}, \bar{\mathbf{k}}) = \frac{|A_o|^2}{d(x_3)} \exp\left[-f_r(x_3)\frac{2x_T^2}{W_o^2} - \gamma_t x_3\right] \delta\left(\bar{\mathbf{k}}_T + f_i(x_3)\frac{2\bar{\mathbf{x}}_T}{W_o^2}\right) \delta\left(k_3 - k_o n' + \frac{df_i(x_3)}{dx_3}\frac{2x_T^2}{W_o^2}\right). \tag{23}$$

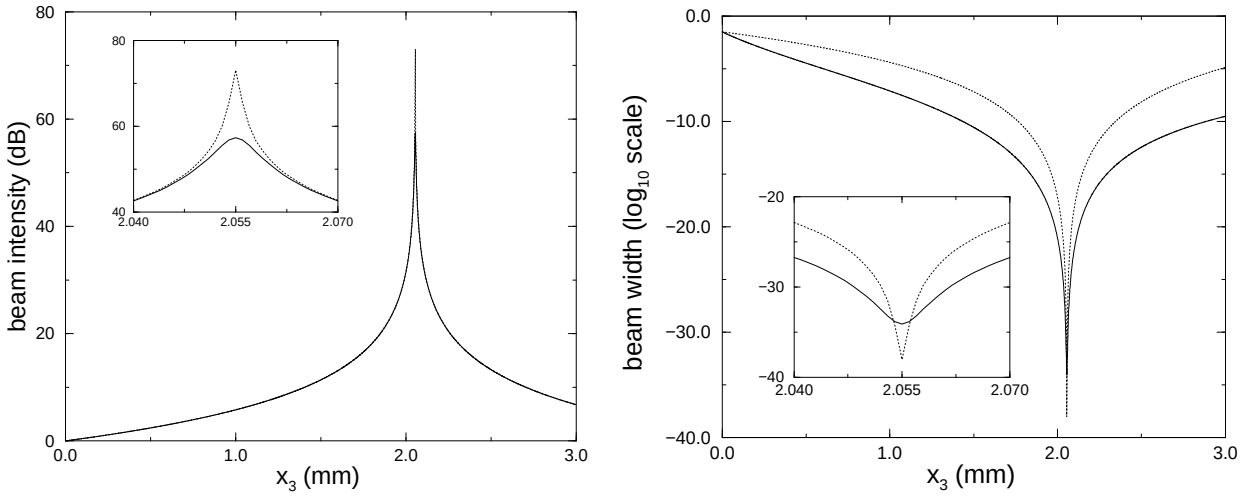

Figure 2. On-axis beam intensity without exponential decay from extinction (left plot) and beam width (right plot) of the Wigner distribution. Here the beam wave parameters are the same as in Figure 1. Dotted lines correspond to propagation free space and solid lines correspond to propagation in a medium with $\gamma_t = 42\,mm^{-1}$. Insets in both plots are close-ups that show the effect of extinction on focusing.

In (23), the argument of the transverse wave-vector distribution leads to the ray path equation,

$$\delta\left(\bar{\mathbf{k}}_T + f_i(x_3)\frac{2x_T}{W_o^2}\right) \qquad \Rightarrow \qquad \bar{\mathbf{k}}_T = k_o \sin\theta = -f_i(x_3)\frac{2x_T}{W_o^2} = \frac{dx_T}{dx_3}. \tag{24}$$

For a particular radial distance given at $x_3 = 0$, the solution to the differential equation above yields the ray path. Some sample ray paths are given in Figure 1. Here, we have chosen the beam wave parameters to correspond to narrow beam waves in biological media.[18] As the extinction coefficient increases, the ray paths deviate from the ray paths in free space and widen the focusing spot size.

From the expression of the Wigner distribution given in (23), we determine the on-axis beam intensity, $b(x_3)$, and the beam width, $w(x_3)$, to be

$$b(x_3) = \frac{|A_o|^2}{d(x_3)}\exp(-\gamma_t x_3) \qquad \text{and} \qquad w^2(x_3) = \frac{W_o^2}{2f_r(x_3)}. \tag{25}$$

In the expression for beam intensity, we easily see that it attenuates exponentially due to extinction. However, in order to fully understand the effect of extinction on the intensity and width, we plot some typical beam intensities (without the exponential decay factor due to extinction) and beam widths in free space and with extinction in Figure 2. As the extinction coefficient increases, deviations the from free space case are seen again near the focal distance that inhibit focusing. In Figure 3 we plot the beam intensity with the exponential decay due to extinction for a variety of extinction coefficients.

3.3. The Reduced Average Intensity

The result for the high-frequency asymptotic Wigner distribution given in (23) is proportional to the reduced intensity of transport theory. Recall that the average intensity is proportional to the energy density,[1]

$$|\phi(\bar{\mathbf{x}})|^2 = \frac{1}{c}\int_{4\pi} I(\bar{\mathbf{x}}, \hat{\mathbf{s}})\, d\Omega(\hat{\mathbf{s}}) = \frac{4\pi}{c}U(\bar{\mathbf{x}}). \tag{26}$$

The asymptotic form of the Wigner distribution in the high frequency limit (16) is easy to integrate over all $\bar{\mathbf{k}}-$space and yields,

$$\int_{I\!R^3} \mathcal{W}(\bar{\mathbf{x}}, \bar{\mathbf{k}}) d^3\bar{\mathbf{k}} = |A(\bar{\mathbf{x}})|^2 = \frac{|A_o|^2}{d(x_3)}\exp\left[-f_r(x_3)\frac{2x_T^2}{W_o^2} - \gamma_t x_3\right] = |\phi(\bar{\mathbf{x}})|^2, \tag{27}$$

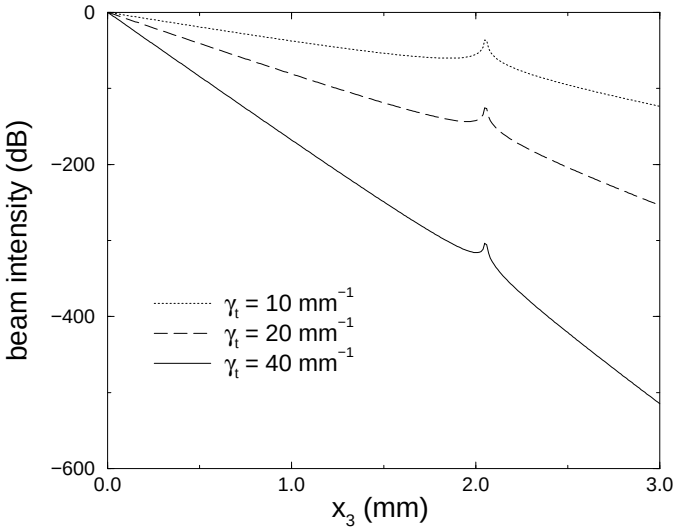

Figure 3. Effect of extinction on the on-axis beam intensity. The beam parameters are the same as figure 1 and 2.

where we have substituted $n'' = \gamma_t/2k_o$. Therefore, we can easily see from these expressions that the average reduced intensity is related the $\bar{\mathbf{k}}-$integrated Wigner distribution by a constant factor of $4\pi/c$.

4. FOCUSED BEAM WAVE DIFFUSION

As a beam wave propagates in a random medium, the reduced intensity exponentially decays due to scattering and absorption. Then the distribution of power that is scattered feeds into diffuse intensity. In a highly scattering medium with little absorption, the average diffuse intensity can be approximated by the diffusion approximation. In this section, we solve the diffusion equation in which the results from previous section are used as source terms.

4.1. Spatial Behavior

To study the spatial behavior of the diffuse average intensity, let us consider the diffusion equation with a continuous wave source,

$$\nabla^2 U(\bar{\mathbf{x}}) - \kappa U(\bar{\mathbf{x}}) = -\eta U_{ri}(x_T, x_3). \tag{28}$$

Here, we define $\kappa = \gamma_a/D$ and $\eta = \gamma_s/D$. To simplify this calculation, we normalize the average reduced intensity, (27) so that it takes on a value of unity at $(x_T, x_3) = (0, 0)$ yielding

$$U_{ri}(x_T, x_3) = \frac{1}{d(x_3)} \exp\left[-f_r(x_3)\frac{2x_T^2}{W_o^2} - \gamma_t x_3\right]. \tag{29}$$

By applying the Hankel transform of order zero on (28), we obtain

$$\frac{\partial^2}{\partial x_3^2}\hat{U}(k_T, x_3) - (\kappa + k_T^2)\hat{U}(k_T, x_3) = -\eta a_o \hat{U}_{ri}(k_T, x_3), \tag{30}$$

where we define the Hankel transform of order zero as

$$\hat{f}(k_T) = \mathcal{H}_o[f(x_T)] = \int_0^\infty dx_T\, x_T\, J_o(k_T\, x_T) f(x_T), \tag{31}$$

and $J_o(x)$ is the Bessel function of order zero. Since the two-dimensional Fourier transform of a radially symmetric function is related to the Hankel transform of order zero by

$$\frac{1}{(2\pi)^2}\int_{I\!R^2} d^2\bar{\mathbf{x}}_T \exp\left[i\bar{\mathbf{k}}_T \cdot \bar{\mathbf{x}}_T\right] f(x_T) = \frac{1}{2\pi}\mathcal{H}_o\left[f(x_T)\right] = \frac{1}{2\pi}\hat{f}(k_T), \tag{32}$$

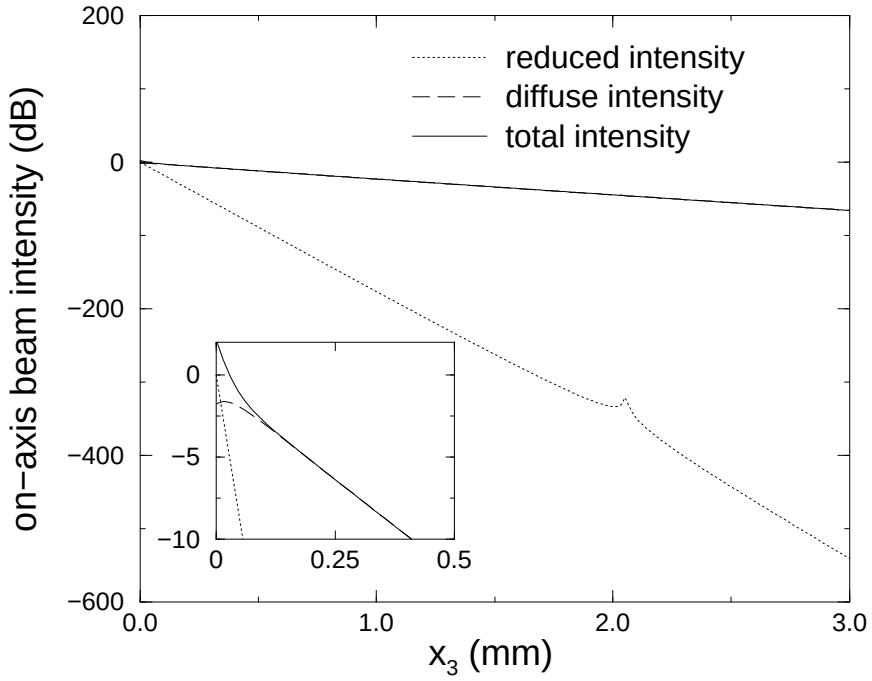

Figure 4. Numerical calculation of the solution of the continuous wave diffusion equation given in (37). This plot shows the on-axis averaged total intensity (solid curve) as well as the reduced intensity (dotted curve). The inset shows a detail of the plot including the average diffuse intensity. Here we consider an albedo value of 0.98 and asymmetry parameter value of 0.80. The other parameters are the same as in Figure 1.

we find that

$$\hat{U}_{ri}(k_T, x_3) = \frac{1}{4}\frac{W_o^2}{d(x_3)f_r(x_3)} \exp\left[-\frac{k_T^2 W_o^2}{8f_r(x_3)} - \gamma_t x_3\right]. \tag{33}$$

Therefore, the solution to (30) is

$$\hat{U}(k_T, x_3) = \int_0^\infty d\zeta\, G(k_T, x_3 - \zeta)\hat{U}_{ri}(k_T, \zeta), \tag{34}$$

where the Green's function,

$$G(k_T, x_3 - \zeta) = \frac{1}{2\sqrt{\kappa + k_T^2}} \exp\left[-\sqrt{\kappa + k_T^2}|x_3 - \zeta|\right] \tag{35}$$

satisfies

$$\frac{\partial^2}{\partial x_3^2} G(k_T, x_3 - \zeta) - (\kappa + k_T^2) G(k_T, x_3 - \zeta) = -\delta(x_3 - \zeta). \tag{36}$$

Here we have assumed that the source function is only non-zero for positive propagation distances. Finally, we can recover the solution in the physical domain by inverse Hankel transforming the result from (34),

$$U(x_T, x_3) = \int_0^\infty dk_T\, k_T\, J_o(k_T\, x_T) \int_0^\infty d\zeta\, G(k_T, x_3 - \zeta)\hat{U}_{ri}(k_T, \zeta) \tag{37}$$

To understand the behavior of the diffuse intensity as it propagates in the medium, we numerically compute the solution given by (37). From our analysis of the reduced intensity, we found that the attenuation due to extinction impeded focusing effects. In the diffusion limit, since directional information of the beam source is lost due to

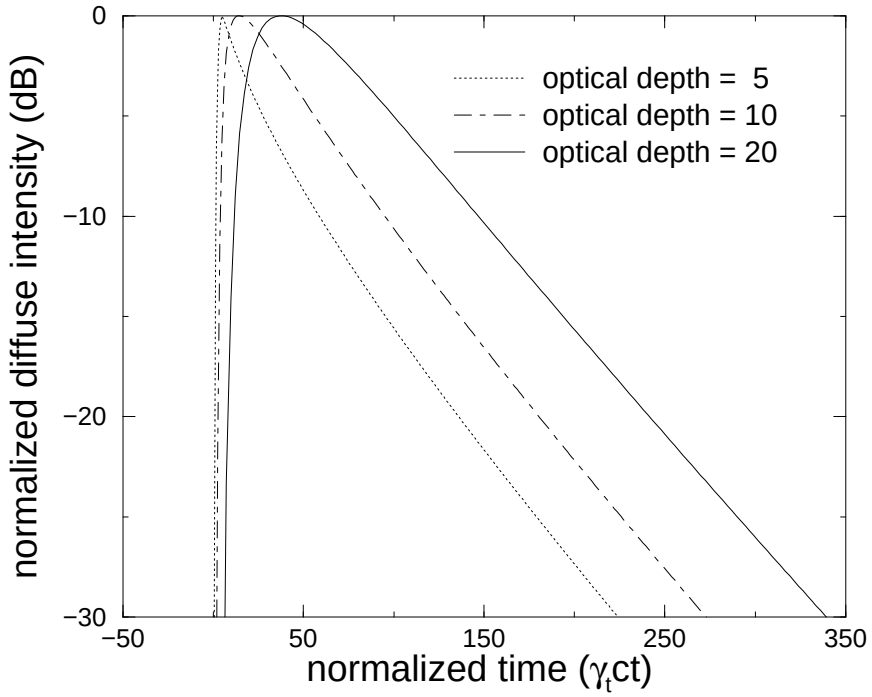

Figure 5. On-axis ($x_T = 0$), average diffuse intensity temporal responses to a delta function input pulse given by (40). These pulse responses are normalized to their peak intensity and plotted on a time scale normalized with the extinction coefficient and constant wave speed as $t/T_o = \gamma_t ct$. For this medium, the albedo value is 0.98 and the asymmetry parameter value is 0.80. The other parameters are the same as in figure 1. These pulse responses are computed at optical depths of 5, 10 and 20 or at approximately $0.12\,mm$, $0.24\,mm$ and $0.48\,mm$, respectively.

significant amounts of multiple scattering, one can expect that focusing would be even more greatly impeded.[19–22] In fact, from our numerical calculations, we find that the effects of focusing on the average diffuse intensity are hardly noticeable. In Figure 4, we show some results from a sample calculation for a medium with albedo equal to 0.98 and mean scattering cosine equal to 0.80. The beam wave parameters for these calculations are the same as the ones used for the reduced intensity study.

In Figure 4, we plot the average total intensity at beam-center as a function of distance. As a reference, we also plot the average reduced intensity at beam-center. The inset of this figure shows the transition that the total intensity makes as the reduced intensity attenuates from scattering and absorption. Although one cannot entirely assume that the diffusion approximation is valid this close to the source, the overall qualitative behavior demonstrated in this figure seems intuitively correct. At the focal length ($\sim 2.055\,mm$ for these particular parameters), the total intensity is effectively equal to the average diffuse intensity since the average reduced intensity suffers from a significant amount of attenuation from scattering and therefore, the diffusing beam does not seem to undergo any focusing effects.

Numerically investigating the spatial spreading as the beam propagates into the medium, we find that beam width increases linearly with propagation distance. This linear growth is a significant departure from the average reduced intensity's beam width (see Figure 2) which spans several orders of magnitude as it propagates in the medium.

4.2. Temporal Behavior

To study the temporal behavior of focused beam wave pulses in a diffusing medium, let us consider the diffusion equation with a delta function input pulse,

$$\frac{1}{c}\frac{\partial}{\partial t}U(x_T, x_3, t) - D\nabla^2 U(x_T, x_3, t) + \gamma_a U(x_T, x_3, t) = \gamma_s U_{ri}(x_T, x_3, t)\delta(t - x_3/c). \tag{38}$$

Here, we are assuming a narrow-band limit whereby the reduced intensity's spectrum is supported locally about the carrier frequency.[4,16] By applying the Fourier Transform on (38), we obtain

$$\nabla^2 U(x_T, x_3, \omega) - (\kappa + i\omega/cD)U(x_T, x_3, \omega) = -\frac{1}{2\pi}\eta U_{ri}(x_T, x_3)\exp(-i\omega x_3/c), \tag{39}$$

where ω is the frequency. Notice that this diffusion equation in the frequency domain takes the same form as (28). Therefore, we can easily write the solution as

$$U(x_T, x_3, \omega) = \int_0^\infty dk_T\, k_T\, J_o(k_T\, x_T) \int_0^\infty d\zeta\, G_c(k_T, x_3 - \zeta, \omega)\hat{U}_{ri}(k_T, \zeta)\exp\left[-i\omega\zeta/c\right], \tag{40}$$

where the Green's function,

$$G_c(k_T, x_3 - \zeta, \omega) = \frac{1}{2\sqrt{\kappa + i\omega/cD + k_T^2}}\exp\left[-\sqrt{\kappa + i\omega/cD + k_T^2}\,|x_3 - \zeta|\right], \tag{41}$$

is a complex function that parametrically depends on frequency. Although some special care must be taken in choosing a branch of the square root functions within the Green's function given above, only a relatively simple modification to the numerical code used to approximation the continuous wave case is needed to consider the pulse case in the frequency domain. Upon computing the spectrum of the diffuse intensity, one can recover the pulse in the time-domain using Fast Fourier Transforms.

As pulses propagate in a scattering medium, one expects that the pulse spreads in time due to scattering.[2] In Figure 5, we plot numerical calculations of (40) along the beam center, $x_T = 0$ at various optical depths. The medium is the same as the one studied in the continuous wave case. The pulse responses have sharp rise and long tails typical of pulses propagating in a diffusing random medium.[16] As pulses propagate deeper into the medium, they undergo a significant amount of temporal spreading. For these calculations we measure the temporal pulse width at $-3\,dB$ below the peak intensity, and find that the pulse spreads nearly linearly with respect to the optical depth.

4.3. Comparison With Collimated Beam and Plane Waves

From the numerical results described above, we find that focused beam wave pulses spread significantly in space and time as they propagate deeper into the medium. Furthermore, these numerical results seem to demonstrate that the effects of focusing in highly-scattering random media are negligible. To fully understand whether focusing effects are evident for focused beam pulses in diffusing media, let us compare the results presented above for spatial spreading to collimated beam waves and temporal spreading to pulsed plane waves.

4.3.1. Collimated Beam Diffusion

To examine spatial spreading, let us revisit the diffusion equation with a continuous collimated beam wave source. Picking up from (30), we examine Hankel transform of the reduced intensity of a collimated beam wave,

$$\hat{U}_{ri}(k_T, x_3) = \frac{1}{4}\frac{W_o^2}{\tilde{d}(x_3)\tilde{f}_r(x_3)}\exp\left[-\frac{k_T^2 W_o^2}{8\tilde{f}_r(x_3)} - \gamma_t x_3\right]. \tag{42}$$

The parameters,

$$\tilde{f}_r(x_3) = \tilde{d}^{-1}(x_3)\left(1 + \frac{x_3}{n' z_o}\frac{\varepsilon}{1+\varepsilon^2}\right) \qquad \text{and} \qquad \tilde{d}(x_3) = 1 + \frac{x_3^2}{n'^2 z_o^2}\frac{1}{1+\varepsilon^2} + 2\frac{x_3}{n' z_o}\frac{\varepsilon}{1+\varepsilon^2}, \tag{43}$$

are evaluated in the collimated beam limit of $R_o \to \infty$. Following Ito[21,22] we assume that the ratio of the extinction coefficient to the wave number is very small which motivates defining the small parameter $\varepsilon = \gamma_t/(2k_o n') \ll 1$. Upon evaluating the asymptotic limit as $\varepsilon \to 0^+$, we obtain,

$$\hat{U}_{ri}(k_T, x_3) \sim \frac{W_o^2}{4}\exp\left[-\frac{k_T^2 W_o^2}{8} - \gamma_t x_3\right] + \mathcal{O}(\varepsilon). \tag{44}$$

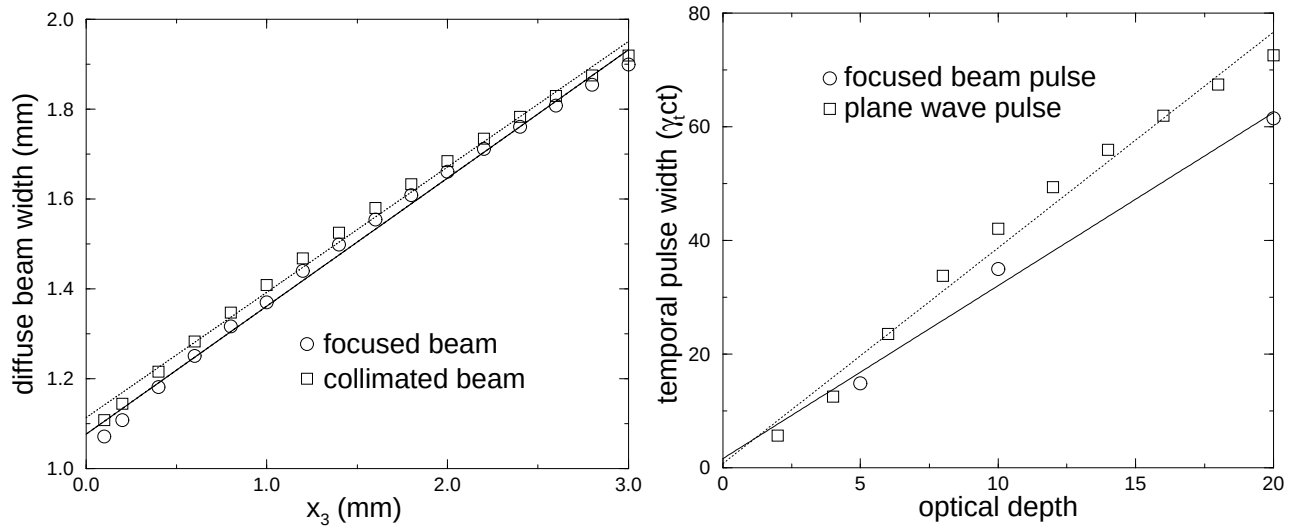

Figure 6. Comparisons of the diffuse intensity's spatial spreading with collimated beams (left plot) and temporal spreading with plane wave diffusion (right plot).

This asymptotic expression greatly simplifies the x_3-dependence in the average reduced intensity, and upon solving (34), we obtain,

$$\hat{U}(k_T, x_3) = \frac{W_o^2}{8\sqrt{\kappa + k_T^2}} \exp\left[-\frac{1}{8}k_T^2 W_o^2\right] \left(\frac{\exp[-\gamma_t z] - \exp[-\sqrt{\kappa + k_T^2}\, z]}{\sqrt{\kappa + k_T^2} - \gamma_t} + \frac{\exp[-\gamma_t z]}{\sqrt{\kappa + k_T^2} + \gamma_t} \right), \tag{45}$$

which can be substituted into (37) to yield the desired solution.

From the previous section, we determined that the focused beam width grows linearly as a function of the propagation distance. We find from numerical calculations that the collimated beam spreads linearly as a function of distance as well. In fact we find that the difference of beam spread of the diffuse component of the focused beam wave defined as

$$\langle x_T^2 \rangle = \int U(x_T, x_3) x_T^2 dx_T \Big/ \int U(x_T, x_3) dx_T \tag{46}$$

from that of the collimated beam is qualitatively negligible. A sample comparison can be seen in the left plot of Figure 6.

4.3.2. Plane Wave Diffusion

To examine temporal spreading, let us reconsider the diffusion equation with a plane wave delta function input source. Starting from (39) with a plane wave source whose reduced intensity is normalized to unity at $x_3 = 0$, we have the following differential equation,

$$\frac{\partial^2}{\partial x_3^2} U(x_3, \omega) - (\kappa + i\omega/cD) U(x_3, \omega) = -\frac{1}{2\pi}\eta \exp\left[-(1 + i\omega/c)x_3\right]. \tag{47}$$

The solution in the frequency domain can be written as

$$U(x_3, \omega) = \frac{\eta}{2\pi} \int_0^\infty d\zeta\, g_c(x_3 - \zeta, \omega) \exp\left[-(1 + i\omega/c)\zeta\right], \tag{48}$$

where

$$g_c(x_3 - \zeta, \omega) = G_c(x_T = 0, x_3, \omega) = \frac{1}{2\sqrt{\kappa + i\omega/cD}} \exp\left[-\sqrt{\kappa + i\omega/cD}\, |x_3 - \zeta|\right] \tag{49}$$

By numerical quadrature and Fourier transform methods, we can compute the resultant solution in the time-domain.

In Figure 6, we compare the temporal spreading of the plane wave pulse to the focused beam wave. Although rates of spreading are different, the spread of the focused beam pulse is qualitatively the same as the plane wave pulse. Therefore, the temporal spread of focused beam wave pulses is qualitatively similar to the temporal spread of plane wave pulses.

5. CONCLUDING REMARKS

In this paper, we have derived a high-frequency asymptotic expression for the reduced intensity of focused beam waves using Wigner distributions. This expression was then used to investigate focused beam pulses in highly scattering media using the diffusion approximation. From the solutions obtained from the diffusion equation, we found that these focused beams spread linearly in space in a similar way to collimated beams and spread linearly in time in a similar way to plane waves.

One aspect of this investigation that was not considered involves addressing the variety of diffusion theories available. Each diffusion theory can yield drastically different results[16] from the others. These discrepancies would most likely get amplified for boundary-value problems since posing physically exact boundary conditions in the diffusion approximation is not always possible and subject to a variety of treatments. In order to address the applicability of the various diffusion theories, we feel that one must closely examine the transition that waves make as they go from a transport theory description to a diffusive one. From understanding this transition, one can diagnostically determine the validity of applying a diffusion approximation and pose physically correct boundary conditions. In future studies, we will address this issue more carefully.

ACKNOWLEDGMENTS

The authors would like to acknowledge their support from the Office of Naval Research, the National Science Foundation and the Army Research Office. A. D. Kim would specifically like to acknowledge his support for this work through a NSF VIGRE research assistantship.

REFERENCES

1. A. Ishimaru, *Wave Propagation and Scattering in Random Media*, IEEE Press, New York, 1997.
2. A. Ishimaru, "Pulse propagation, scattering and diffusion in scatterers and turbulence," *Radio Science* **14**(2), pp. 269–276, 1979.
3. S. Chandrasekhar, *Radiative Transfer*, Dover, New York, 1960.
4. A. Ishimaru, "Diffusion of a pulse in densely distributed scatterers," *J. Opt. Soc. Am.* **68**, pp. 1045–1050, 1978.
5. A. Ishimaru, "Diffusion of light in turbid material," *Appl Opt.* **28**(12), pp. 2210–2215, 1989.
6. K. Furutsu, "Diffusion equation derived from space-time transport equation," *J. Opt. Soc. Am.* **70**(4), pp. 360–366, 1980.
7. M. C. W. van Rossum and T. M. Nieuwenhuizen, "Multiple scattering of classical waves: microscopy, mesoscopy, and diffusion," *Rev. Mod. Phys.* **71**(1), pp. 313–371, 1999.
8. A. Yodh and B. Chance, "Spectroscopy and imaging with diffusion light," *Physics Today* , pp. 34–40, March 1995.
9. E. Wigner, "On the quantum correction for thermodynamic equilibrium," *Physical Review* **40**, pp. 749–759, June 1932.
10. H. Bremmer, "General remarks concerning theories dealing with scattering and diffraction in random media," *Radio Science* **8**(6), pp. 511–534, 1973.
11. R. Fante, "Relationship between radiative-transport theory and maxwell's equations in dielectric media," *J. Opt. Soc. Am.* **71**, pp. 460–468, 1981.
12. L. Ryzhik, G. Papanicolaou, and J. B. Keller, "Transport equations for elastic and other waves in random media," *Wave Motion* **24**, pp. 327–370, December 1996.
13. S. Ito, "Comparison of diffusion theories for optical pulse waves propagated in discrete random media," *J. Opt. Soc. Am. A* **1**(5), pp. 502–505, 1984.
14. A. Ishimaru, "Difference between ishimaru's and furutsu's theories on pulse propagation in discrete random media," *J. Opt. Soc. Am. A* **1**(5), pp. 506–509, 1984.

15. A. Polishchuk, S. Gutman, M. Lax, and R. Alfano, "Photon-density modes beyond the diffusion approximation: scalar wave diffusion," *J. Opt. Soc. Am. A* **14**(1), pp. 230–234, 1997.
16. A. D. Kim and A. Ishimaru, "Optical diffusion of continuous-wave, pulsed, and density waves in scattering media and comparisons with radiative transfer," *Appl. Opt.* **37**(22), pp. 5313–5319, 1998.
17. A. Ishimaru, *Electromagnetic Wave Propagation, Radiation and Scattering*, Prentice Hall, Englewood Cliffs, New Jersey, 1991.
18. M. Keijzer, S. Jacques, S. Prahl, and A. Welch, "Light distributions in artery tissue: Monte carlo simulations for finite diameter laser beams," *Appl. Opt.* **28**(12), pp. 2331–2336, 1989.
19. A. Ishimaru, Y. Kuga, R. Cheung, and K. Shimizu, "Scattering and diffusion of a beam wave in randomly distributed scatters," *J. Opt. Soc. Am.* **73**(2), pp. 131–136, 1983.
20. J. Ying, F. Liu, and R. Alfano, "Spatial distrubtion of two-photon-excited fluorescence in scattering media," *Appl. Opt.* **38**(1), pp. 224–229, 1999.
21. S. Ito, "Diffusion of collimated, narrow beam waves in discrete random media," *Appl. Opt.* **34**(30), pp. 7106–7112, 1995.
22. S. Ito, "Theory of beam light pulse propagation through thick clouds: effects of beamwidth and scatterers behind light source on pulse broadening," *Appl. Opt.* **20**(15), pp. 2706–2715, 1995.